

Probabilistic vibration and lifetime analysis of regenerated turbomachinery blades

Ricarda Berger*, Timo Rogge, Eelco Jansen and Raimund Rolfes

Leibniz Universität Hannover, Institute of Structural Analysis, Appelstraße 9A, 30167 Hanover, Germany

(Received June 15, 2016, Revised August 9, 2016, Accepted August 12, 2016)

Abstract. Variances in turbomachinery blades caused by manufacturing, operation or regeneration can result in modified structural behavior. In this work, the scatter of geometrical and material properties of a turbine blade and its influence on structure performance is discussed. In particular, the vibration characteristics and the lifetime of a turbine blade are evaluated. Geometrical variances of the surface of the blades are described using the principal component analysis. The scatter in material properties is considered by 16 varying material parameters. Maximum vibration amplitudes and the number of load cycles the turbine blade can withstand are analyzed by finite element simulations incorporating probabilistic principles. The probabilistic simulations demonstrate that both geometrical and material variances have a significant influence on the scatter of vibration amplitude and lifetime. Dependencies are quantified and correlations between varied input parameters and the structural performance of the blade are detected.

Keywords: aeroengine; probabilistic analysis; structural analysis; starting dynamics; lifetime

1. Introduction

Components of aircraft engines have to meet increasingly high requirements. Especially bladings crucial for safe engine operation are exposed to high loads. The failure of one single blade usually leads to the loss of all downstream stages and therefore has a severe impact on the availability of the aeroengine. In the design process, the properties of the nominal blade are determined, taking into account the aerodynamic and structural requirements. Advanced numerical simulation methods such as the widely-used finite element method provide the possibility to predict the behavior of the structure.

However, in reality the properties of the blade will definitely differ from the ones assumed during the design process. Manufacturing processes, operation and maintenance lead to scattering structural properties in every component. Consequently, each single blade behaves differently, corresponding to its own specific scattering properties. In order to ensure safety of the structure on the basis of deterministic analysis overly conservative assumptions have to be made. In a probabilistic analysis, the consequences of uncertainties are no longer covered by safety factors and structures are characterized depending on scattering parameters. Basic ideas to incorporate probabilistic methods in turbomachinery design processes are given by Vogeler and Voigt (2015).

*Corresponding author, Ph.D. Student, E-mail: r.berger@isd.uni-hannover.de

A main benefit of including probabilistic principles is the increase in understanding of complex structural behavior.

An essential prerequisite for successfully using probabilistic tools is a proper characterization of variances. The challenge is therefore to capture the different kind of scattering parameters appropriately.

In recent years, much progress has been made in detecting and modeling the scatter in geometrical properties caused by manufacturing variability. Garzon and Darmofal (2003) and Lange *et al.* (2012) investigated the geometrical scatter in airfoils of compressor blades in a probabilistic setting using computational fluid dynamic (CFD) simulations. Turbine blades geometries are parameterized and analyzed by Heinze *et al.* (2013). Further parametric models for airfoils are given by Heinze (2015), who used aerodynamical parameters to describe variances of the surface. The effect of geometrical variances due to operation and overhaul are evaluated by Hohenstein *et al.* (2013) mapping geometrical variances on a profile of a turbine blade.

Variances in material properties in terms of material anomalies are considered by Enright *et al.* (2006), who performed probabilistic fracture mechanical analysis on aeroengine components. Also, Fei *et al.* (2015) quantified the radial deformation of turbine blades incorporating the density of the blade as a random variable.

The primary aim behind analyzing turbomachinery structures within a probabilistic framework is to quantify the effect of variances on aerodynamic performance and structural behavior. Extensive studies on changes in aerodynamic efficiency of axial compressors are made by Lange (2016). Furthermore, the structural analysis of blades can be divided into dynamic analysis and life estimation.

Hou and Wicks (2002) investigated the influence of root flexibility and untwist effects on the vibration of turbine blades in numerical simulations and series of tests. The vibration behavior of rotor blades resulting from geometrical variances of upstream vanes are presented by Aschenbruck *et al.* (2013b). In addition, Vogeler and Voigt (2015), Booyesen *et al.* (2015) and Aschenbruck *et al.* (2013a) also provided findings on varying natural frequencies and eigenmodes of turbine blades.

Besides dynamic properties, the estimation of service life is another major task of structural analysis. A simple method to evaluate fatigue failures is proposed by Hou *et al.* (2002), who analyzed the steady-state stresses and dynamic characteristics under typical failure conditions. Booyesen *et al.* presented a probabilistic approach to predict the lifetime of a steam turbine blade using a cumulative damage formulation. The comparison of various damage theories for the determination of fatigue failure and service life is given by Rao *et al.* (2001).

This present work focuses on the dynamics and fatigue of turbine blades, which are found in an axial air-turbine (Aschenbruck *et al.* 2013a). A series of computations is performed to determine the vibration amplitudes during start up and the failure cycle. Thereby, the influence of geometrical and material variances on the structural parameters is considered. To make the time-consuming simulations feasible for stochastic analysis the approaches developed by Rogge and Rolfes (2012) and applied for failure analysis by Holl *et al.* (2014) are used.

2. Geometrical and material variances

For modeling geometrical and material variances measurement data and data from literature has to be prepared. The different treatment of uncertainties in geometrical and material properties is discussed in the following.

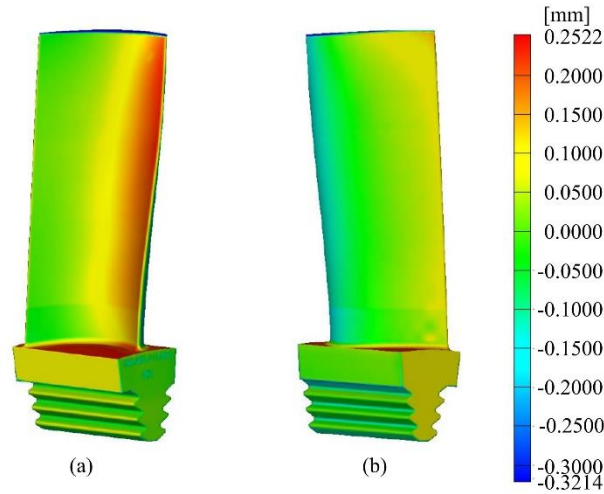


Fig. 1 Evaluated deviations between measured and ideal geometry of one turbine blade using GOM Inspect viewed (a) from the front and (b) from the back

2.1 Geometrical variances

The geometrical variability due to manufacturing tolerances can be measured by optical three-dimensional scanner. Variances in the surfaces of 20 rotor blades are detected using an optical scanner with an accuracy of 0.01 mm. The data of the individual blade geometry is then available as a randomly distributed point cloud. The CAD-model of the ideal blade geometry is taken as a reference. Deviations between ideal and real geometry are evaluated using the software GOM Inspect (GOM 2016), as shown in Fig. 1. Subsequently the surface data are mapped on the final FE-model.

According to the resolution of the mesh used for structural analysis, the extracted data sets are high-dimensional. The data set $\mathbf{X} \in \mathbb{R}^{n \times p}$ comprises n observations (here $n = 20$) and p dimensions (here number of nodes on the surface) and is assumed to be normally distributed. The dimensionality can be reduced significantly by applying a Principal Component Analysis (PCA), as given by Jolliffe (2002). The PCA allows converting the data into a new set of fewer independent variables and is therefore a common method to describe geometrical variances of turbomachinery blades.

In order to apply the PCA to the prepared measured data the standardized data set $\mathbf{X}_s \in \mathbb{R}^{n \times p}$ is used. For this, matrix \mathbf{X} is centered with the average $\vec{\bar{x}}$ and normalized with the standard deviation \vec{s} of n data sets. The matrix \mathbf{X}_s with n standardized vectors $\vec{x}_{s,n}^T$ is given by

$$\mathbf{X}_s = \begin{bmatrix} \vec{x}_{s,1}^T \\ \vdots \\ \vec{x}_{s,n}^T \end{bmatrix} \quad (1)$$

The factorization of \mathbf{X}_s by singular value decomposition (SVD) leads to the matrix \mathbf{U} , the diagonal matrix \mathbf{S} and the matrix of eigenvectors \mathbf{V}^T

$$\mathbf{X}_s = \mathbf{USV}^T \quad (2)$$

Thereby, the matrix of amplitudes related to the eigenvectors is given by

$$\mathbf{A} = \mathbf{US} \quad (3)$$

The diagonal entries $(\sigma_1, \dots, \sigma_r)$ of matrix \mathbf{S} are known as the singular values of \mathbf{X}_s which correspond to the eigenvalues of the PCA through $\sigma_r^2 = \lambda_r$. The number of eigenvalues is determined by $r = \text{rank}(\mathbf{X}_s)$. The standard deviation of eigenvectors is given by

$$s_r = \sqrt{\frac{\lambda_r}{n-1}} \quad (4)$$

Finally, the standardized data sets can be written as a linear combination of eigenvectors \vec{v}_i with the corresponding amplitudes a_i linked to the matrix of amplitudes \mathbf{A}

$$\vec{x}_s = \sum_{i=1}^r a_i v_i \quad (5)$$

A further reduction of dimensionality is achieved by assuming that the first l eigenvectors are sufficient to describe the essential characteristics of the blade geometry and all subsequent vectors have a negligible influence. The number of eigenvectors to be included is determined using the following criterion

$$\sum_{i=1}^l \left(\frac{\lambda_i}{\sum \lambda_i} \right) > \kappa \quad (6)$$

with $\kappa = 0.95$. The criterion is fulfilled if the sum of the scatter of eigenvalues contains 95 % of the entire scatter. The number of eigenvectors considered is reduced from r to l . According to Fig. 2 in the particular example only 13 instead of 19 eigenvectors have to be considered.

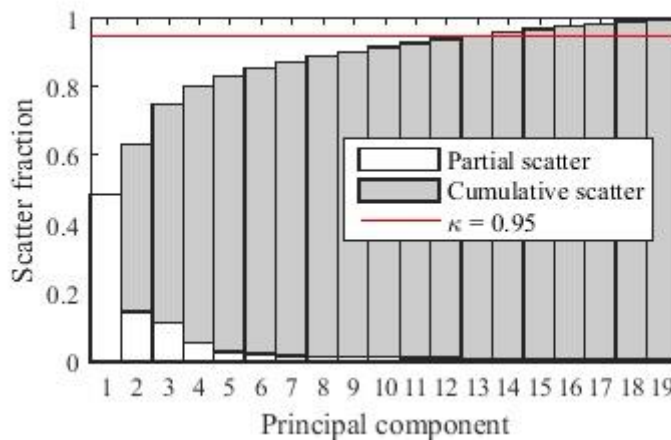


Fig. 2 Fraction of scatter explained by each principal component

Table 1 Varying material parameters of Certal EN AW 7022

Parameter	Unit	Mean μ	Standard deviation σ
Density	P kg/m ³	2759.38	39.625
Young's modulus	E MPa	72000	1447.545
Poisson's ratio	N	0.33	0.0243
Thermal expansion coefficient	A 1/K	0.00002368	0.00000029
Thermal conductivity	λ W/mK	135.13	5.0417
Specific heat capacity	c_p J/kgK	862.27	13.6584
Damping ratio	D	0.0011	0.000287
Yield strength	R_p MPa	493	9.0106
Tensile strength	R_m MPa	550	6.8793
Uniform strain	E	0.068	0.005
Activation energy of primary creep	A_{prim} J/mol	12260	1021.2735
Strain hardening coefficient of primary creep	n_{prim}	1.4026	0.3632
Activation energy of secondary creep	A_{sec} J/mol	138110	11504.8299
Strain hardening coefficient of secondary creep	n_{sec}	4.6100	1.1942
Fatigue strength	N kN/m ²	16200	2256.756
Creep strength	T kN/m ²	5410	678.0155

Subsequently, within the probabilistic analysis simply l uncorrelated scattering variables a_i instead of p variables have to be varied. The normal distribution function of the amplitudes is defined by the mean $\bar{a}_i = 0$ and the standard deviation s according to Eq. (4).

2.2 Material variances

The turbine blades analyzed are made out of high strength aluminum alloy (Certal EN AW 7022). The specification of the scatter of the corresponding material parameters is based on data available in the literature (e.g., ThyssenKrupp 2016, Brenner 1956).

Mechanical properties (Young's modulus, yield strength, tensile strength and uniform strain) are measured in tensile tests. Moreover, all 16 material properties are assumed to be normally distributed and the mean values and standard deviations are given in Table 1.

3. Computational model

For the analysis of the starting dynamics and for the fatigue analysis, a finite element model of the rotor blade is developed. In order to minimize the computation time in the probabilistic analysis, several simplifying approaches are introduced.

3.1 Finite element model

The CAD-model of a single rotor blade is meshed with fully integrated tetrahedron elements with quadratic shape functions. Tetrahedral elements are used due to the complex geometry of the

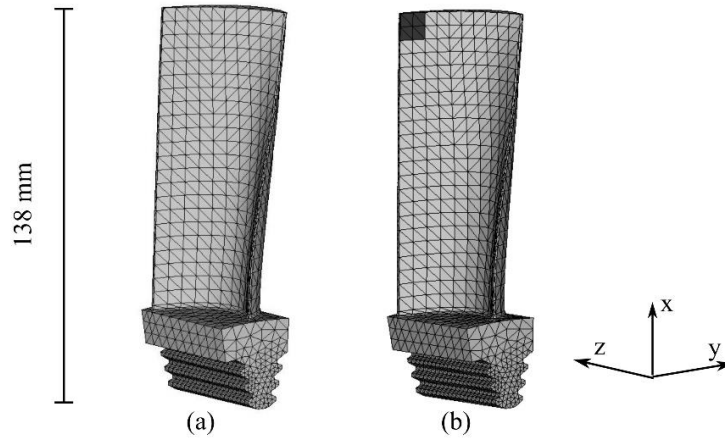


Fig. 3 Finite element mesh of the turbine blade investigated (a) without repair and (b) with patch

structure. Generally, the local density of the mesh applied to the blade is higher at the blade root than at the top edge. Thereby the failure, which is expected to occur in the fir-tree region, can be captured accurately. In total, the finite element model of the blade as it is shown in Fig. 3(a) and (b) comprises about 19600 nodes and about 11900 elements. In addition, in Fig. 3(b) a regenerated turbine blade with a patch at the trailing edge is depicted.

Furthermore, the boundary conditions at the blade root are simplified. During operation, the forces are transferred to the disk via the contact between the upper flanks of the fir-tree teeth and the groove. To avoid time-consuming contact computations the degrees of freedom of the displacement field of the upper flanks of the fir-tree are constrained in x and y -direction. To fix the model in z -direction displacement constraints in z -direction are applied to the nodes located in the mid plane of the blade root.

The material characteristics of the aluminum alloy are described by a visco-elasto-plastic material law. The material model used includes a bilinear stress-strain behavior with kinematic hardening as well as a linearized creep law considering the primary and secondary creep stages. The tangent modulus for the material law considering the plastic material behavior above the yield point with tensile strength R_m , yield strength R_p , elongation at break ε_B and Young's modulus E is given by

$$E_T = \frac{R_m - R_p}{\varepsilon_B - \frac{R_p}{E}} \quad (7)$$

In this way the thermo-mechanical material behavior of the blade is modeled sufficiently accurate.

3.2 Operating conditions and load assumptions

In the different phases of one flight profile, the aeroengine passes various operating points and thus the turbine blades are subjected to different external loads. For the purpose of efficient

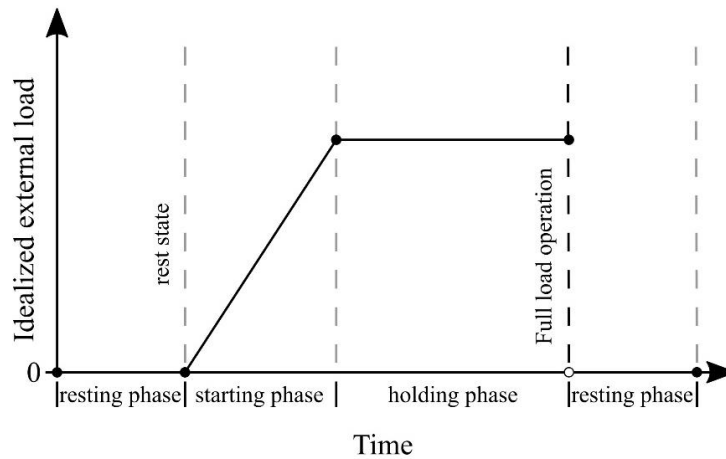


Fig. 4 Computation cycle for one flight operation

computation, a basic computation cycle shown in Fig. 4 is generated on the basis of decisive operating points in time.

One flight cycle is subdivided in a starting phase and a holding phase of full load operation. The starting phases are of particular importance for dynamic analysis, because the increasing rotational speed leads to different excitations. The holding phases are significant for estimating lifetime. Each flight operation is accompanied by pre- and post-operational resting phases that correspond to the periods without external loading. In total, a complete flight operation of an aircraft engine can be described by this simplified computation cycle.

The operational loads of the turbine blade consist of centrifugal forces, gas forces and thermal loads. The centrifugal forces vary according to the rotational speed and can be described quasi-statically for each operating point.

The time-dependent aerodynamic gas forces lead to the main excitation, which takes place at the nozzle passing frequency. This frequency is given by the product of rotational speed with the number of upstream blades or vanes. The dynamic force component of the gas forces is estimated from the static force component of the gas forces due to the proportionality to the empirical stimulus (Traupel 2001).

The temperature and flow fields of the fluid are computed in stationary CFD simulations for significant operating points. The conditions between the operating points are approximated by linear interpolation. The thermal load of the blade is determined assuming purely convective heat transfer between gas and structure. The temperature field within the structure thereafter results from heat distribution by conduction.

All further computations are performed for a turbine blade of the 5th stage of the air-turbine of the Institute of Turbomachinery and Fluid Dynamics (TFD) of Leibniz Universität Hannover (Aschenbruck *et al.* 2013a). The operating conditions and external loads of the blading are shown in Table 2.

3.3 Probabilistic model

For performing structural analysis incorporating probabilistic principles the commercial

Table 2 Operating parameters of the 5th stage blading of the axial air-turbine

Description	Value
Max. rotational speed	7500 rpm
Max. gas temperature	332 K
Max. static pressure	121 kPa
Resting time	8.375 h
Starting time	0.75 h
Holding time	5 h

software OptiSLang is used. The designs analyzed in numerical simulations are generated using Latin Hypercube Sampling (LHS). The mean value and the standard deviation of normally distributed geometrical or material parameters are considered. In total three different configurations of the gas turbine blades are investigated. Firstly, geometrical variances of the surface due to manufacturing are considered. Secondly, the scatter of material parameters is analyzed. Finally, the influence of a patch repair on the turbine blade is simulated. The analysis of starting dynamics and fatigue life of the modified blades is performed. Main output parameters of the probabilistic model therefore are the frequencies at resonance point, the maximum vibration amplitude and the number of cycles the structure can resist before structural failure is reached. Conclusively, correlations between parameters and distributions of output parameters are determined in post-processing routines using Matlab.

4. Analysis of starting dynamics

During run-up of the engine the operating conditions change and hence the vibration behavior changes. The frequencies and vibration amplitudes, which characterize the dynamic behavior, are analyzed subsequently. The results computed within the deterministic analysis correspond to a blade with nominal global material properties.

4.1 Deterministic analysis

Due to the increasing rotational speed, gas forces and temperatures during the starting phase, no constant natural frequencies can be assumed. The natural frequencies corresponding to different rotational speeds are computed by modal analysis including pre-stress based on linear eigenvalue analysis. The eigenmodes are associated with the natural frequencies using the Modal Assurance Criterion (MAC). The relevant three natural frequencies of the rotor blade in the operating range between 0 to 7500 rpm are analyzed in a deterministic simulation. The frequencies and the corresponding first bending mode in flapwise direction, the first torsional mode and the first bending mode in edgewise are depicted in Fig. 5. Furthermore, no significant dependence between the increased centrifugal loads and the natural frequencies is observed in this particular example. The primary reasons for this are the relatively low loads and the conservative design of the blades.

The excitation of the rotor blade is directly associated with the nozzle passing frequency. As the 5th stage of the air-turbine is composed of 29 vanes, the major excitation frequency in the Campbell diagram (Fig. 5) is given by the 29th engine order (EO). Potential resonance conditions

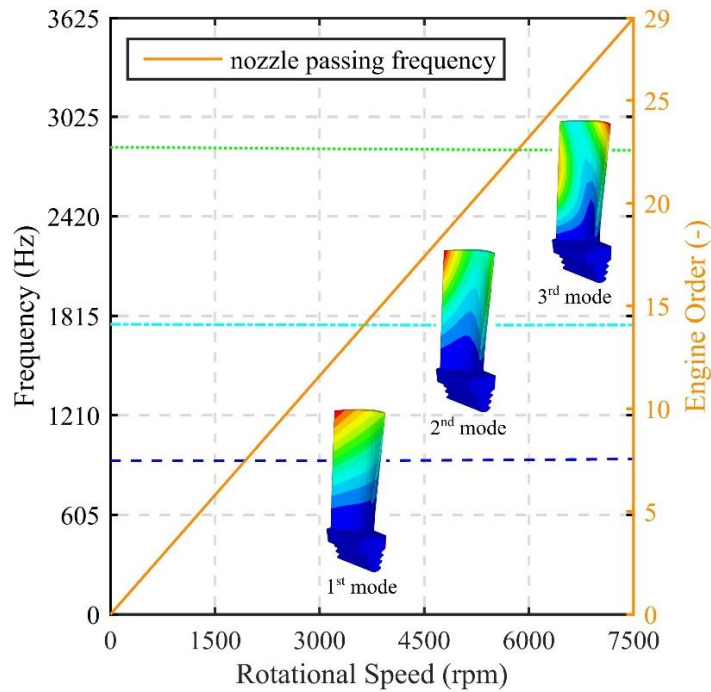


Fig. 5 Campbell diagram of the rotor blades investigated

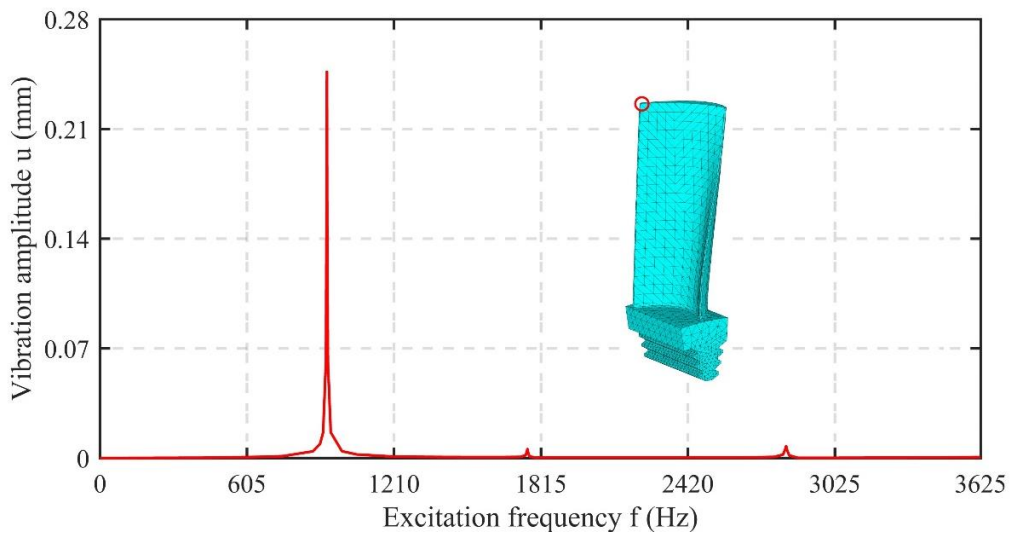


Fig. 6 Frequency response analysis of the rotor blades investigated

are identified where natural frequencies of the blade and the EO line coincides. In this particular example, the resonance points are at frequencies of 929.56, 1752.92 and 2818.28 Hz.

Besides the resonance frequencies, the vibration amplitudes are investigated. The frequency response analysis performed is based on the approximation approach presented by Rogge and

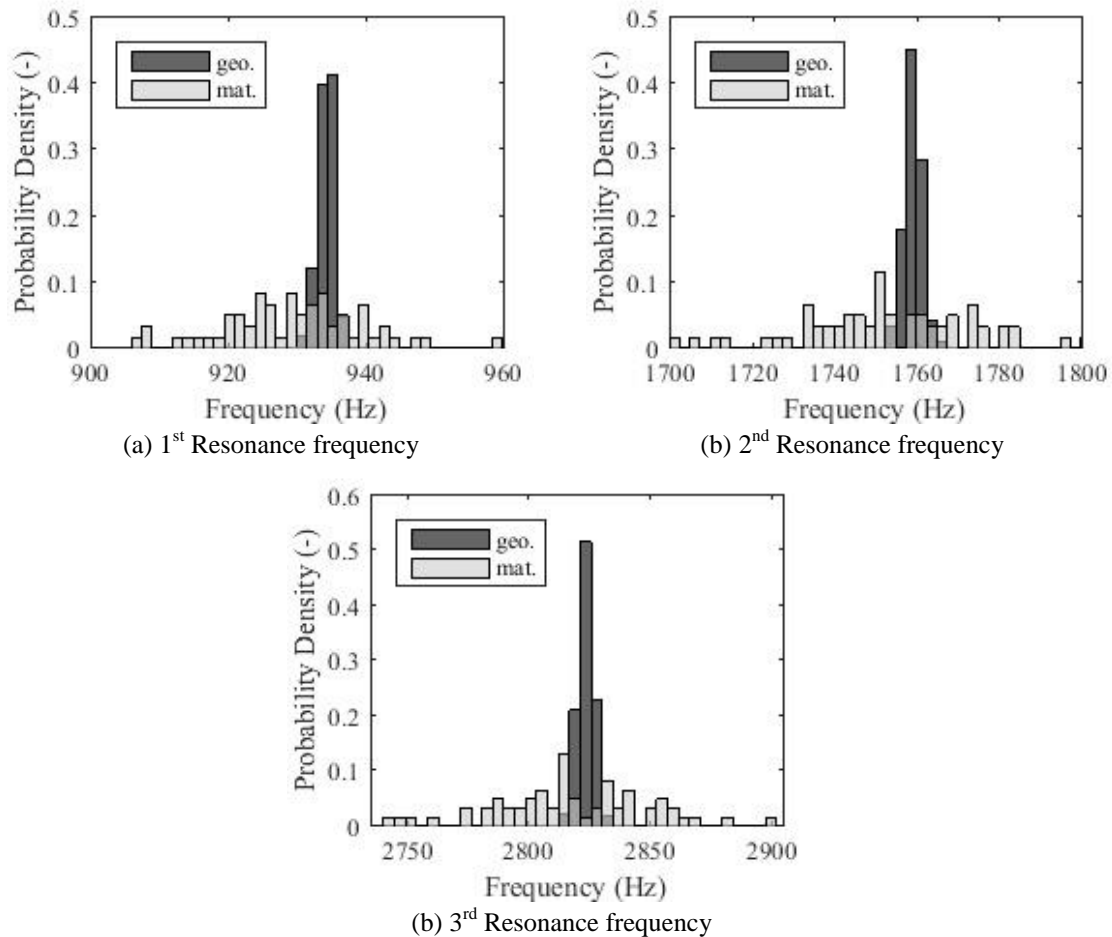


Fig. 7 Scatter of resonance conditions due to scatter in geometrical (geo.) and material (mat.) parameters

Rolfes (2012). Since frequency response analysis is limited to stationary conditions assuming a steady state, the vibration amplitude is approximated by a superposition of partial frequency responses calculated at supporting points. Each partial frequency response is computed using modal superposition and frequency-clustering. The final frequency response as it is depicted in Fig. 6 results from the superposition of partial frequency responses by linear weighting functions.

As an example, the absolute value of resulting vibration amplitudes of a node located at the trailing edge next to the blade tip. are shown in Fig. 6. The results of this particular node are depicted, because there the highest vibration amplitudes can be observed. Especially the excitation corresponding to the lowest natural frequency leads to higher vibration amplitudes, in this specific case of 0.254 mm. The vibration amplitude at the other resonance points is relatively small.

4.2 Probabilistic analysis

Within the probabilistic analysis, firstly the dependence of the resonance frequencies on the

geometrical and material properties of the blade is considered. The computational results of 250 samples are shown in Figs. 7(a)-(c). The histograms of the three resonance frequencies calculated take into account either geometrical or global material variances. The scatter of frequencies illustrates the influence of varying properties. In general it can be concluded, that the material parameters have a significantly higher influence on the structural response properties than the geometrical uncertainties. The scatter of resonance conditions caused by material variability is higher and causes a broader distribution. Nevertheless, the scatter in input parameters in both cases leads to almost normally distributed resonance frequencies. The resonance frequencies computed in deterministic simulation lies within the stochastic distribution caused by variances. A general trend or shift of resonance frequencies in a certain direction due to the scatter in material parameters cannot be detected. The averaged resonance frequencies are in agreement with the values of the deterministic analysis. Furthermore, the geometrical variances lead to a small shift of about 5 up to 7 Hz towards higher resonance frequencies.

The influences of the geometrical and material variances on the maximum vibration amplitude u_{max} are shown in Figs. 8 and 9. As can be seen from the cumulative distribution function (Fig. 8) the maximum vibration amplitudes of a rotor blade with geometrical imperfections may vary in a range between 0.24 and 0.254 mm. The distribution of the output parameter can be again assumed to be a normal distribution as the comparison with the theoretical function (using a mean value of 0.2471 mm and a standard deviation of the sample of 0.0017 mm) shows.

The distribution of maximum vibration amplitudes caused by material variances is however clearly not normally distributed (Fig. 9). The graph of the cumulative distribution function indicates a distribution with positive skewness. Thus, the combination of different material properties on average leads to maximum vibration amplitudes in the range around 0.25 mm. In many cases, the vibration amplitudes influenced by material variability are larger than the amplitudes predicted with geometrical variances. In general, the scatter due to changes in material properties is again larger than the influence of variable geometry.

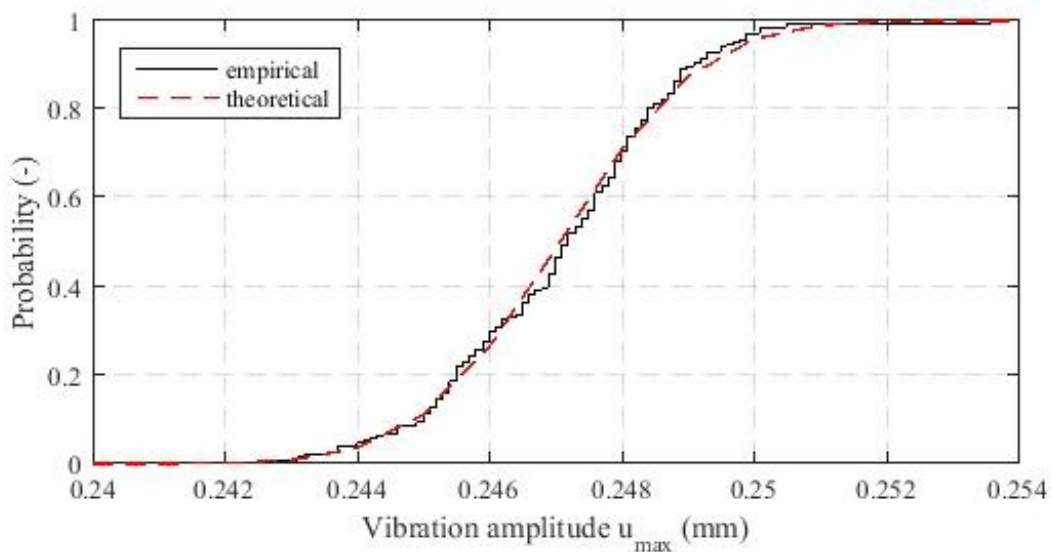


Fig. 8 Variance in maximum vibration amplitudes caused by variable geometrical parameters

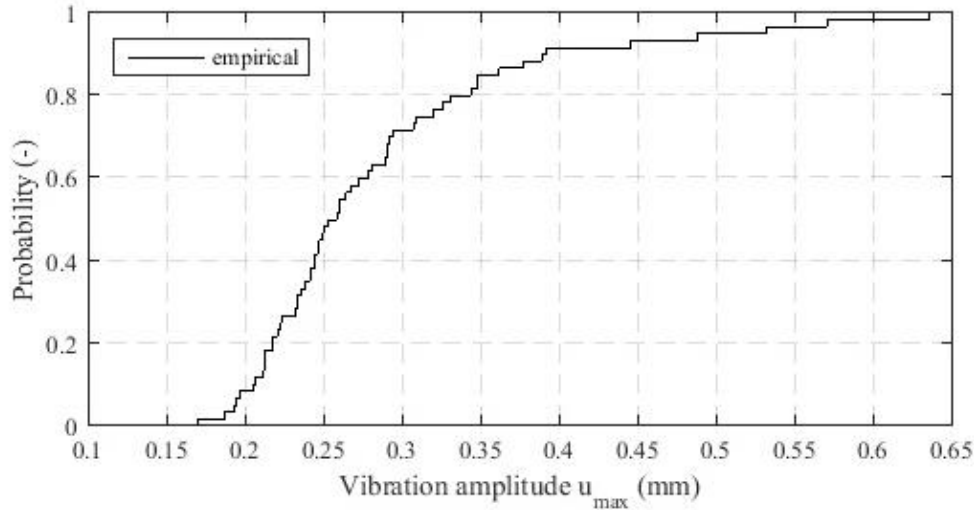


Fig. 9 Variance in maximum vibration amplitudes caused by variable material parameters

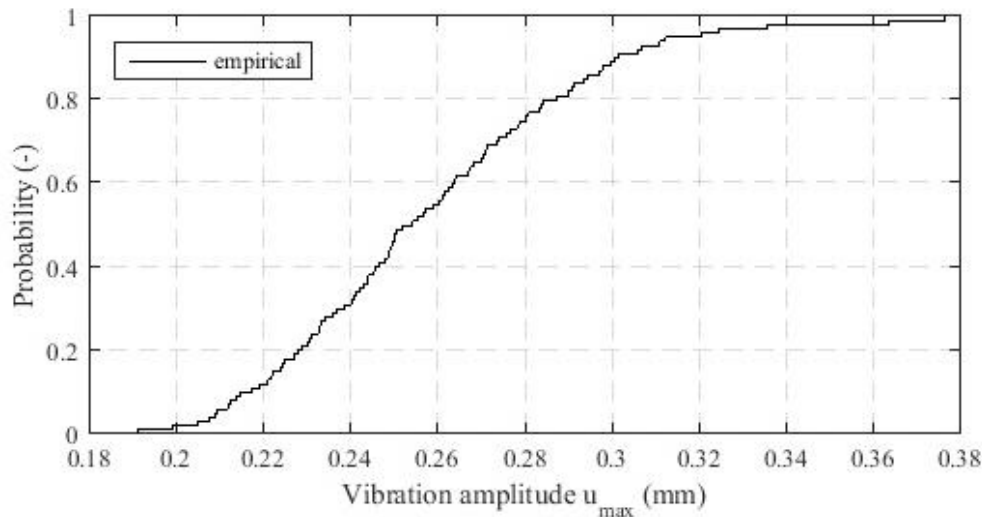


Fig. 10 Variance in maximum vibration amplitudes caused by variable material parameters of the patch

Furthermore, the cumulative distribution of vibration amplitudes computed with the regenerated turbine blade is shown in Fig. 10. Material properties are varied according to Table 1. Due to the scattering material properties of the patch material added at the blade tip maximum vibration amplitudes occur in the range between 0.18 and 0.38 mm. Again, the scatter caused by the material variability of the patch is significantly larger than the scatter caused by geometrical variances. Moreover, it can be found that the results determined within the simulation of the regenerated blade lie within the range of vibration amplitudes specified in the analysis with varying global material parameters.

In order to quantify the dependence between the input and output parameters used within the numerical simulations the correlations are investigated. To measure the correlation the rank

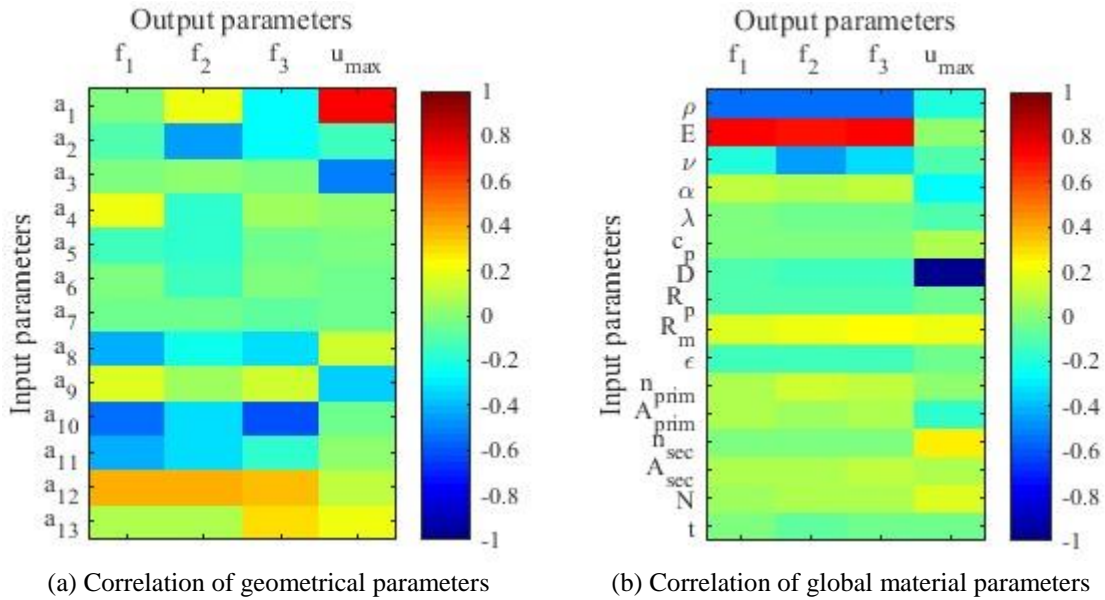


Fig. 11 Spearman rank correlation of input and output parameters of starting dynamics

correlation coefficients proposed by Spearman (1904) are used. The correlation between input parameters and previously introduced output parameters of the starting dynamics are shown in Figs. 11(a)-(b).

The correlation matrix in Fig. 11(a) illustrates that the amplitudes a_{10} corresponding to the 10th eigenvector have the highest influence on the resonance frequencies. A general in- or decrease in influence of the amplitudes associated with their order cannot be found. In contrast, the maximum vibration amplitudes are dominated by the influence of the first eigenvector. The Spearman rank correlation coefficient has a value of 0.722.

Regarding the influence of the material parameters, a significant correlation between the density of the blade and the Young’s modulus with the resonance conditions is identified in Fig. 11(b). In accordance with physical considerations, an increase of mass leads to lower natural frequencies and vice versa, a higher Young’s modulus results in higher natural frequencies. The correlation matrix also shows the influence of damping on the maximum vibration amplitudes. An increase of the damping of the structure directly results in reduced vibration amplitudes. As expected the thermal material properties only have a negligible influence on the resonance frequencies. Similar correlation can be found between the properties of the material of the patch placed on the regenerated blade and the output parameters. The correlations correspond to the correlations of scattering global parameters (Fig. 11(b)).

5. Analysis of lifetime

For the determination of the lifetime of the turbine blade, the entire service life of the aircraft engine has to be considered. The damage the turbine blade suffered during various flight operations is analyzed in a deterministic analysis. Further, the importance of different variances is

evaluated by stochastic characteristics.

5.1 Deterministic analysis

The prediction of the failure cycle of the turbine blade is relatively time consuming, because the simulation for one flight cycle has to be repeated many times. In view of this, the simulation time of one simulation run has to be reduced as much as possible. Therefore, the damage of the blade is predicted using the semi-analytical approach developed by Rogge and Rolfes (2012).

The approach is based on a linear damage accumulation model according to Palmgren-Miner (Miner 1945). Additionally the damage caused by creep is considered by an additional term as given by Sabour and Bhat (2008). Hence, the total damage with the fatigue contribution D_f and creep contribution D_c is defined as

$$D_{tot} = D_f + D_c \quad (7)$$

According to the cumulative rule, the damage is determined dependent on the stresses and temperatures the blade has to resist in each load cycle and summed up to get the current damage. The particular advantage of including the semi-analytical approach lies in the reduction of the computation time through analytical estimation of stresses. In this approach, the assumption of a quasi-stable state is introduced. After this state has been reached, the stresses in the subsequent cycles are assumed to behave linearly. The damage no longer needs to be computed numerically and the simulation time is reduced drastically.

The progression of total damage and its contributions for the location of maximum damage is shown in Fig. 12. As depicted, a typical damage pattern can be found and the failure of the blade occurs in the fir-tree. Moreover, only the damage up to 1% of failure is considered in order to reduce computational time. The exact number of cycles, which leads to failure, can be extrapolated linearly. In this particular example, the rotor blade fails after 6712 flight cycles. Due to relatively low temperatures, the contribution of creep is low as compared to the one caused by fatigue.

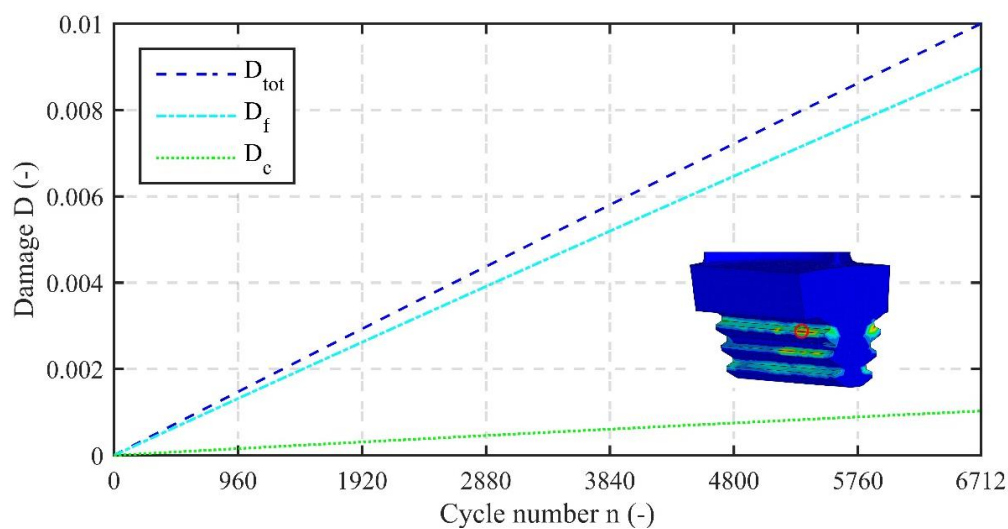


Fig. 12 Maximum local damage within the rotor blades

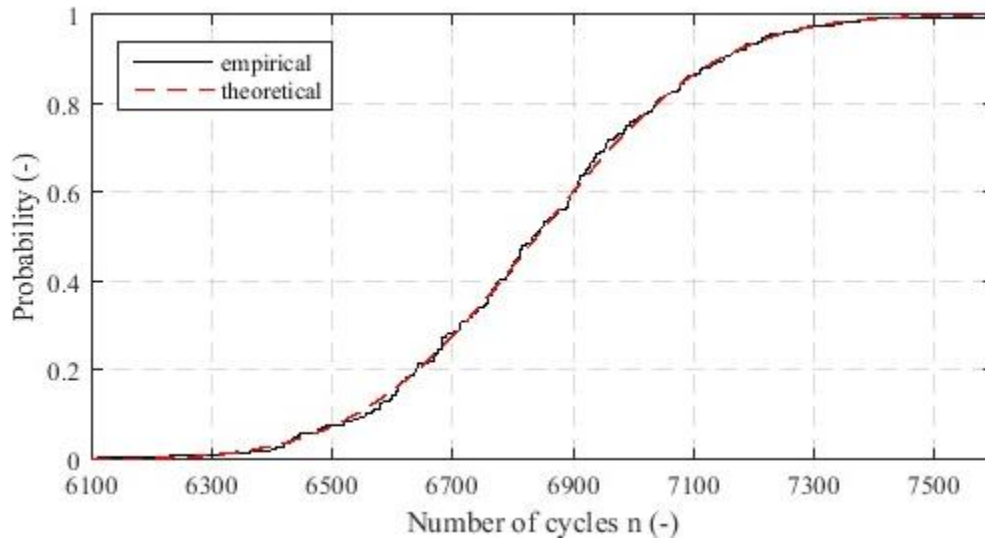


Fig. 13 Variance in lifetime caused by variable geometrical parameters

5.2 Probabilistic analysis

In the designs evaluated, the influence of geometrical variances on the failure cycle n is described by a cumulative distribution function (Fig. 13). Again a damage level of $D_{tot} = 0.01$ is used for the determination of the number of cycles the structure is able to resist. A theoretical normal distribution function is shown and compared with the empirical distribution. It can thus be concluded that the number of cycles resulting from scatter in geometry is normally distributed with a mean value of about 6840 cycles.

The scatter in global material parameters finally leads to large deviations within the estimated lifetime. According to the cumulative distribution function of the flight cycles n shown in Fig. 14, some blade designs can be loaded over 220000 cycles before 1% of total damage is reached. In some cases, long lifetime is estimated although the variance of material properties at the same time leads to higher vibration amplitudes (Fig. 9). However, often the combination of the uncorrelated material properties encourage high fatigue strength. Thus, the influence of higher vibration amplitudes is relatively low as compared to superior material properties. The grey colored area illustrates that the range of estimated lifetime caused by geometrical uncertainties is relatively small as compared to the scatter in lifetime caused by varying material properties. Nevertheless, more than 50% of the samples lies within this range (see zoomed figure). The coefficient of variation of the distribution of lifetime $c_v = \frac{\text{standard deviation}}{\text{mean}}$ of 1.8 indicates the large scatter of output parameters. In comparison, the maximum variation coefficient which can be found for the modal damping is only 0.26. Accordingly, the scatter of lifetime is significantly larger than the scatter in each material parameter. Besides that, the output parameter does not follow a normal distribution, as was the case with geometrical variances.

The correlation between the different input parameters and the number of flight cycles is measured by the Spearman rank correlation coefficients. According to this, the scatter of the 2nd amplitude primary influences the lifetime of the rotor blade (Fig. 15(a)). The influence of all other

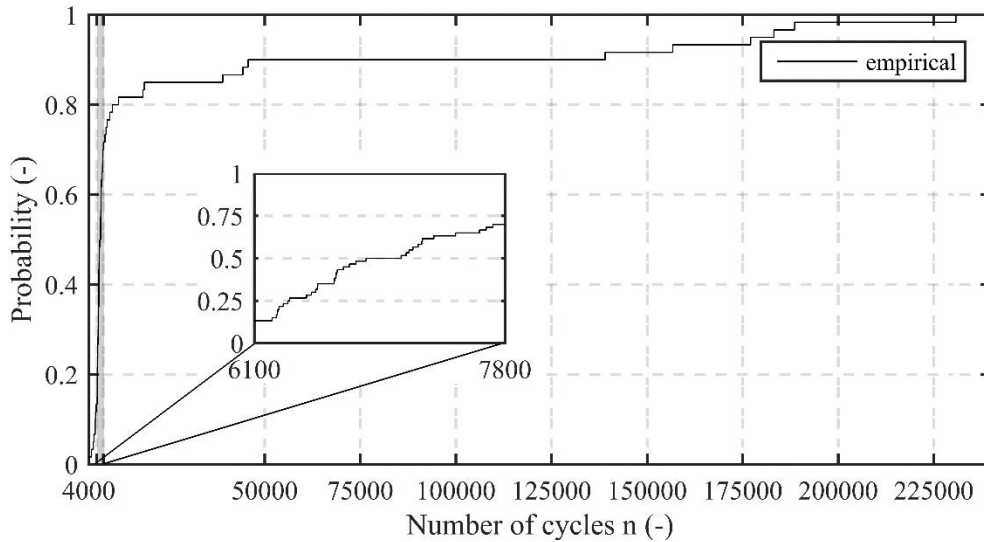
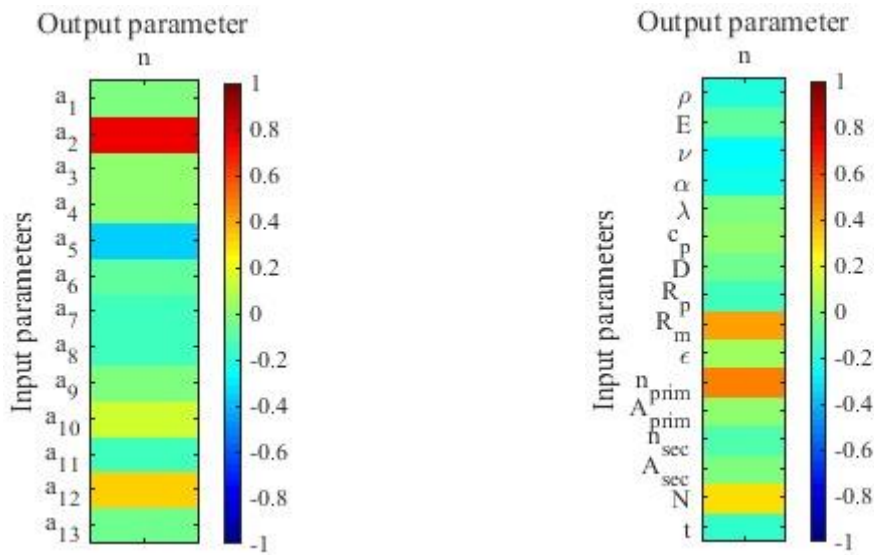


Fig. 14 Variance in lifetime caused by variable material parameters



(a) Correlation of geometrical parameters

(b) Correlation of material parameters

Fig. 15 Spearman rank correlation of input and output parameters of lifetime analysis

amplitudes is comparatively small.

Considering the material parameters the failure cycle is mainly influenced by the tensile strength R_m and the strain hardening coefficient of primary creep n_{prim} which are directly incorporated in the calculation of characteristic values used within the computation of the fatigue damage.

6. Conclusions

In the present paper, the influence of typical scattering parameters on the structural behavior of a turbine blade is investigated. Significant geometrical and material parameters are specified and transferred to the blades of an axial air-turbine. Variances in the geometry of the structure are measured with 3D optical scanners and described on the basis of principal components determined in a PCA. Material uncertainties are given by 16 parameters, which correspond to a typical scatter of material properties found in the literature. A finite element model of a single blade is used within the structural analysis. Incorporating the approach proposed by Rogge and Rolfes (2012) allows a fast evaluation of the structure. Thereby especially the starting dynamics and the lifetime of gas turbines blades are analyzed in detail.

Natural frequencies and corresponding resonance conditions are determined and critical maximum vibration amplitudes are obtained by frequency response analysis. In the deterministic example, the maximum vibration amplitudes are about 0.25 mm and result from the excitation by the nozzle passing frequency. Simulating various load cycles, the damage suffered is investigated. The total damage according to cumulative damage theory of Palmgren-Miner and Robinson leads to the number of cycles the blade can resist before failure occurs. Within the deterministic simulation, a damage level of 1% is reached after about 6700 flight cycles and the location of maximum damage is detected in the fir-tree.

Furthermore, the probabilistic framework allows to evaluate the effects of the scatter found in geometrical and material properties. The probabilistic analysis demonstrates that both variances in structural properties lead to significant scatter of vibration characteristics and predicted lifetime. Maximum vibration amplitudes up to 0.254 mm are computed due to geometrical variances and a variation of material properties results in amplitudes of almost 0.65 mm. The range of estimated lifetime of blades including geometrical variances goes from 6100 up to 7800 cycles. Considering a variation of material properties for blades, the number of cycles until a 1% damage level is damaged even reaches the high number of 225000. Hence, it can be found that the influence of scattering material parameters is dominantly responsible for changes in the structural behavior of the blade. Comparing the coefficients of variation of the distribution of material input parameters to the coefficients related to the distribution of lifetime it can be concluded, that the scatter in output parameters is even higher than the scatter in material input.

In addition, the evaluation of the Spearman rank correlation matrices allows the description of dependencies between structural properties and dynamic and fatigue parameters analyzed. The vibration amplitudes are strongly affected by the first eigenvector of the PCA and the modal damping applied. The number of flight cycles until a certain level of damage is dominantly influenced by the second eigenmode as well as the tensile strength and the strain hardening coefficient of primary creep behavior.

Further steps will include the structural analysis of various regeneration-induced variances caused by different repair techniques and strategies and their effect on the vibration and lifetime of the regenerated blades.

Acknowledgments

The support of the German Research Foundation (DFG, Deutsche Forschungsgemeinschaft) through its Collaborative Research Centre (SFB, Sonderforschungsbereich) 871-Regeneration of

Complex Capital Goods is gratefully acknowledged.

References

- Aschenbruck, J., Adamczuk, R., and Seume, J.R. (2014), "Recent progress in turbine blade and compressor blisk regeneration", *Proceedings of the 3rd International Conference on Through-life Engineering Services*, Cranfield, England, November.
- Aschenbruck, J., Meinzer, C.E. and Seume, J. (2013b), "Influence of regeneration-induced variances of stator vanes on the vibration behaviour of rotor blades in axial turbines", *Proceedings of the 10th European Conference on Turbomachinery Fluid dynamics & Thermodynamics*, Lappeenranta, Finland, April.
- Aschenbruck, J., Meinzer, C.E., Pohle, L., Panning-von Scheidt, L. and Seume, J. (2013a), "Regeneration-induced forced response in axial turbines", *Proceedings of the ASME Turbo Expo 2013*, San Antonio, Texas, USA, June.
- Booyens, C., Heyns, P.S., Hindley, M.P. and Scheepers, R. (2015), "Fatigue life assessment of a low pressure steam turbine blade during transient resonant conditions using a probabilistic approach", *Int. J. Fatig.*, **73**, 17-26.
- Brenner, P. (1956), "Statische und dynamische Festigkeitseigenschaften hochfester Aluminiumlegierungen", *Aluminium*, **32**, 756-768
- Enright, M.P., Hudak, S.J. and McClung, R.C. (2006), "Application of Probabilistic fracture Mechanics to Prognosis of Aircraft engine components", *AIAA J.*, **44**(2), 311-316.
- Fei, C., Tang, W., Bai, G. and Ma, S. (2015), "Dynamic probabilistic design for blade deformation with SVM-ERSM", *Aircraft Eng. Aerosp. Tech.*, **87**(4), 312-321.
- Garzon, V.E. and Darmofal, D.L. (2003), "Impact of geometric variability on axial compressor performance", *Proceeding of the ASME Turbo Expo 2003*, Atlanta, Georgia, USA, January.
- GOM (2016), available online at: <http://www.gom.com> (accessed 3 August 2016).
- Heinze K., Meyer M., Scharfenstein J., Voigt, M. and Vogeler, K. (2013), "A parametric model for probabilistic analysis of turbine blades considering real geometric effects", *CEAS Aeronaut. J.*, **5**(1), 41-51.
- Heinze, K. (2015), "Eine Methode für probabilistische Untersuchungen zum Einfluss von Fertigungsstreuungen auf die hochzyklische Ermüdung von Verdichterschaufeln", Ph.D. Dissertation, TU Dresden, Dresden.
- Hohenstein, S., Aschenbruck, J. and Seume, J. (2013), "Einfluss betriebs- und regenerationsbedingter Varianzen von Turbinenschaufeln", *Int. J. Elect. Heat Gen. VGB Power Tech.*, **11**, 51-58.
- Holl, M., Rogge, T., Loehnert, S., Wriggers, P. and Rolfes, R. (2014), "3D multiscale crack propagation using the XFEM applied to a gas turbine blade", *Comput. Mech.*, **53**(1), 173-188.
- Hou, J. and Wicks, B.J. (2002), "Root flexibility and untwist effects on vibration characteristics of a gas turbine blade", Defence Science and Technology Organization Victoria (Australia) Platform Science Lab, No. DSTO-RR-0250.
- Hou, J., Wicks, B.J. and Antoniou, R.A. (2002), "An investigation of fatigue failures of turbine blades in a gas turbine engine by mechanical analysis", *Eng. Fail. Anal.*, **9**(2), 201-211.
- Jolliffe, I. (2002), *Principal Component Analysis*, 2th Edition, Springer, New York, NY, USA.
- Lange, A. (2016), "Performanceuntersuchung eines Hochdruckverdichters unter Berücksichtigung geometrischer Variabilität", Ph.D. Dissertation, TU Dresden, Dresden.
- Lange, A., Voigt, M., Vogeler, K. and Johann, E. (2012), "Principal component analysis on 3D scanned compressor blades for probabilistic CFD simulation", *53rd AIAA/ASME/ASCE/AHS/ASC Structures, Structural Dynamics and Materials Conference Honolulu*, Hawaii.
- Lange, A., Voigt, M., Vogeler, K., Schrapp, H., Johann, E. and Gümmer, V. (2012), "Impact of

- manufacturing variability on multi-stage high-pressure compressor performance”, *Proceedings of the ASME Turbo Expo 2012*, Copenhagen, Denmark.
- Miner, M.A. (1945), “Cumulative damage in fatigue”, *J. Appl. Mech.*, **12**(3), 159-164.
- Rao, J.S. (2000), *Turbine blade life estimation*, 1st Edition, Alpha Science International, Pangbourne, UK.
- Reyhani, M.C., Alizadeh, M., Fathi, A. and Khaledi, H. (2013), “Turbine blade temperature calculation and life estimation-a sensitivity analysis”, *Propuls. Power Res.*, **2**(2), 148-161.
- Rogge, T. and Rolfes, R. (2012), “Stochastische Untersuchungen regenerationsbedingter Imperfektionen einer Turbinenschaufel-Modellierung des deterministischen Modells zur effizienten Berechnung des Schwingungs- und Festigkeitsverhaltens”, *Proceedings of 5 Dresdener-Probabilistik-Workshop*, Dresden, Germany, October.
- Sabour, M.H. and Bhat, R.B. (2008), “Lifetime prediction in creep-fatigue environment”, *Mater. Sc. Poland*, **26**(3), 563-584.
- Spearman, C. (1904), “The proof and measurement of association between two things”, *Am. J. Psychol.*, **15**(1), 72-101.
- ThyssenKrupp (2016), “Data sheet: EN AW-7022”, available online at: http://www.thyssenkrupp.ch/documents/Al_Platten_7022.1.pdf (accessed 3 August 2016).
- Traupel, W. (2001), *Thermische Turbomaschinen II*, 4th Edition, Springer, Berlin, Germany.
- Vogeler, K. and Voigt, M. (2015), “Probabilistic analysis of complex system behavior in turbomachinery design”, *Proceedings of International Gas Turbine Congress*, Tokyo, Japan, November.